World Academy of Science, Engineering and Technology
International Journal of Mechanical and Mechatronics Engineering
Vol:16, No:8, 2022

Predictions of Dynamic Behaviors for Gas Foil Bearings Operating at Steady-State Based on Multi-Physics Coupling Computer Aided Engineering Simulations

Tai Yuan Yu, Pei-Jen Wang

Open Science Index, Mechanical and Mechatronics Engineering Vol:16, No:8, 2022 publications.waset.org/10012649.pdf

***Abstract*—**A simulation scheme of rotational motions for predictions of bump-type gas foil bearings operating at steady-state is proposed. The scheme is based on multi-physics coupling computer aided engineering packages modularized with computational fluid dynamic model and structure elasticity model to numerically solve the dynamic equation of motions of a hydrodynamic loaded shaft supported by an elastic bump foil. The bump foil is assumed to be modelled as infinite number of Hookean springs mounted on stiff wall. Hence, the top foil stiffness is constant on the periphery of the bearing housing. The hydrodynamic pressure generated by the air film lubrication transfers to the top foil and induces elastic deformation needed to be solved by a finite element method program, whereas the pressure profile applied on the top foil must be solved by a finite element method program based on Reynolds Equation in lubrication theory. As a result, the equation of motions for the bearing shaft are iteratively solved via coupling of the two finite element method programs simultaneously. In conclusion, the two-dimensional center trajectory of the shaft plus the deformation map on top foil at constant rotational speed are calculated for comparisons with the experimental results.

***Keywords*—**Computational fluid dynamics, fluid structure interaction multi-physics simulations, gas foil bearing, load capacity.

I. INTRODUCTION

BECAUSE gas foil bearings (GFB) are designed to operate in high rotational speed, high gas temperature and lubricant free environment, they are superior in life-span and maintenance costs to both rolling-element bearings and hydrodynamic oil bearings. Walowit and Anno [1] first published the fundamental theory of bump type GFB and improved simulation schemes for predictions of GFB performances and characteristics. Due to the complex mechanical design of the support structure on bump foil, the difficulty in predictions of GFB performances has increased accordingly. In the literature, pertinent design factors, such as bump foil deformation, interfacial forces between the top foil and bump foil, and top foil deformation induced by gas pressure profile, have to be carefully examined and assessed for improvement on the prediction accuracy. The elastic material properties of bump foil critically influence the stiffness of the GFB; hence, it must be characterized for the effects on GFB performances.

Heshmat et al. [2] presented an analytic model for simulating the steady state behaviors of bump type GFBs. To achieve the goal of accurate model in simulating the dynamic performances of the GFB, Ku and Heshmat [3] reported a theoretical model with considerations of the interaction forces, friction forces and geometric factors for prediction of the coefficients of stiffness and damping of bump foil attached to top foil. Agrawal [4] summarized the development history and category of major GFBs. Among the categories, the GFBs with multiple leaf top foil structure and the GFBs with corrugated bump type top foil structure are dominant more recently because of their outstanding working performance and compact structure. Although the elastic characteristics of bump foil structure can increase the stability of GFB, there is still dilemma in selection of the stiffness of bump foil structure. Hence, balance of high load capacity and high damping factor to maintain high stability in bum foil structure is more difficult as compared with leaf-type foil bearings.

Iordanoff [5] illustrated a simplified model to analyze the stiffness and steady state behaviors of bumps foil of GFBs. The results indicated that the compliance parameters of the free bumps and welded bumps have to be represented by two formulae. DellaCorte and Valco [6] classified all GFBs into three generations by the structure characteristics via a simple classification method. The conclusion showed the feasibility in estimation of GFB load capacity based on some published experimental data. Therefore, the bump type GFBs with similar bump structures have been the highlighted topics of research in more recent years.

In general, the bump type GFBs are characterized by two main components, namely the top foils acting as the smooth supporting bearing surface and a deformable corrugated bump foils under the top foil serving as the supportive springs. Not only could the bump foils provide elastic support forces but also induce frictional damping effects due to friction surface interactions. The schematics of the configuration of bump-type GFBs are shown in Fig. 1.

Tai Yuan Yu and Pei-Jen Wang are with the National Tsing Hua University, No. 101, Sec. 2, Guangfu Rd., East Dist., Hsinchu City., Taiwan R.O.C. (e-mail: www6112000@gmail.com, pjwang@pme.nthu.edu.tw).

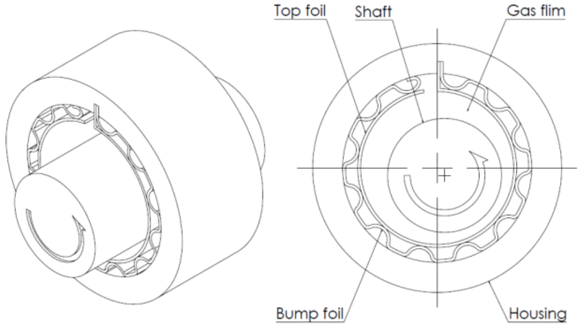

Fig. 1 3-D projective and 2-D schematics of bump-type GFB; main parts including top foil, bump foil, shaft and housing with circular arrow indicating the shat rotational direction

Carpino and Talmage [7] derived a complete formulation by using the coupled Finite Element Method with consideration of the shape of gas film, effects due to bending of the top foil, deformations of radial and circumferential direction of the bump foil. To estimate the load capacity of the GFB, a comprehensive simulation model is necessary. Peng and Khonsari [8], [9] assumed the uniform deformation of the foils structure along the axial direction of the shaft and proposed a simulation model with the stiffness of GFB in a structural compliance coefficient representing the material and configuration of bump foil. Furthermore, Swanson [10] presented a simplified model of the bump foils by substitution of each bump by two springs connected to rigid links. San Andres and Kim [11] introduced a numerical analysis model that considered the local deformation of the bump foil structure and top foil simulation by two parts in finite element models, a 1D beam structure and a 2D shell. In addition, the friction forces generated by the interactions of the bumps and the housing are also considered. To accurately estimate the deformation of the foil structure of GFBs, Le Lez et al. [12], [13] presented a method based on the large displacement theory for approximation of the effective interactions between the foils by Finite Element Method. Feng and Kaneko [14] later presented a theoretical model for multiple foil structure by considering the local deformation of the top foil. On the other hand, Lee et al. [15] provide a method for analysis of the dynamic and static performances and characteristics of bearings.

The objective of this paper is to establish a numerical simulation model for bump-type GFBs including all factors such as interaction forces, stiffness of bumps, local deformation of the top foil and friction forces between foils. As a result, the proposed simulation model would predict the effects of friction forces and interaction forces in the foils. Deformation of the top foil can be approximated by plate and shell theories; and, the stiffness of bump foil can be calculated by the Finite Element Method. Since the fundamental theory of GFBs is based on multi-physics domain, the pressure distribution along the shaft, shaft vibrations, and bump foil deformation would influence the GFB performances. It is essential to put focus on the methodology to establish fluid-structure coupling simulation model for the GFBs to predict the load capacity under steady state operation conditions. A three-dimensional commercial computer aided engineering (CAE) analysis package, copyrighted by Ansys Inc., USA, with built-in multi-physics simulation capability is employed for the investigation in GFBs. The results would give pressure and temperature profiles and load distributions data that could be used for experimental verifications in the future.

II. NUMERICAL SIMULATION ANALYSIS MODEL OF GFB

A. *Introduction of Multi-Physics Coupling Simulation Method*

To analyze the dynamic behavior of GFBs during the high rotation speed, building a model which can simulate and predict the motion characteristic of GFB during operating is necessary. However, the top foil and the bump foil are both kinds of elastic material. As a result, the shape of gas film exists in the clearance between the high-speed moving surface of the shaft and the high frequency vibrating surface of top foil. They will change during the GFB process. Meanwhile, as a response to the gas film deformation caused by the deflection foil, the foil surface will be reshaped by the pressure which has already been rearranged in the gas film. This interaction relationship between fluid field and structure will not converge to a certain steady state completely. Therefore, predicting the operating characteristic of GFB by steady state analysis is insufficient for real cases. To improve the consistency of the analytical model and the real model, the analytical model has to consider the coupling model with two way calculation. To achieve the above objective, it is necessary to establish analytical models including the interactions both for gas film and foil structure to simulate the dynamic behaviors of GFB at high rotational speed by the finite element method. In this study, a commercial multi-physics package, copyrighted by Ansys Inc., consisting of computational fluid dynamics module called CFX and transient structural module is employed for the simulations.

Because the simulation of the dynamic characteristic and working behavior involves complicated multi-physics analysis including hydrodynamic, transient structure and heat transfer at interface, two simulation modules are paralleled connected to form a complete simulation model which is solved iteratively to give the simulated results. This multi-physics coupling simulation model can be set to initialize the boundary conditions both in the thermal fluid and structure module individually. Later, the simulation is conducted with the data exchange of the different field interface to make the simulation converge to the solutions of characteristics of GFBs operating at steady state. The method of the analytical data exchange among solvers' interfaces uses the calculated results of one solver model as the boundary conditions for the other solver model iteratively. The time steps of the two modules can be selected by a higher coupling module to complete the simulation as illustrated in Fig. 2 for details.

B. *Numerical Simulation Analysis Model of GFB in Gas Film*

We build a model to analyze the status of the characteristics of the fluid. To achieve that, we built a hollow circle column 3D geometry model to simulate the shape of the fluid field of

GFB. The environmental pressure and temperature can be set on the front and back surface of the GFB model. That setting can not only define the interface fluid condition in bearing clearance but also simulate the heat transfer effect caused by the convection of fluid appearing there. After that, the surface velocity caused by the effect of the high-rotation speed shaft can be directly achieved by setting the surface rotation velocity value on the inner surface of the GFB model to do the simulation. On the other hand, due to the outside surface of the working fluid in bearing clearance is top foil so the tangential velocity is zero there. However, the heat transfer phenomenon not only appears on the front and back interface but also happens on the outside and inside the surface of the fluid field. To include that effect in the simulation model, we also set the heat transfer boundary condition on the outside surface. It can help us to estimate that phenomenon by setting the target temperature and the heat transfer coefficient of the contact object surface, see Fig. 3 for details.

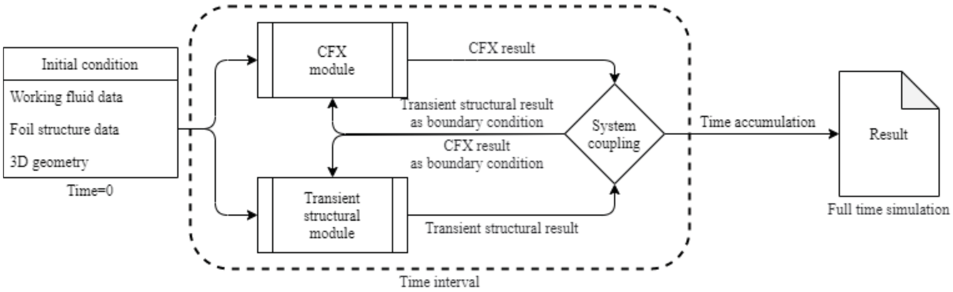

Fig. 2 Work-flow schematic of proposed multi-domain coupled CAE simulations on air foil bearings; dashed block indicating the coupling modules

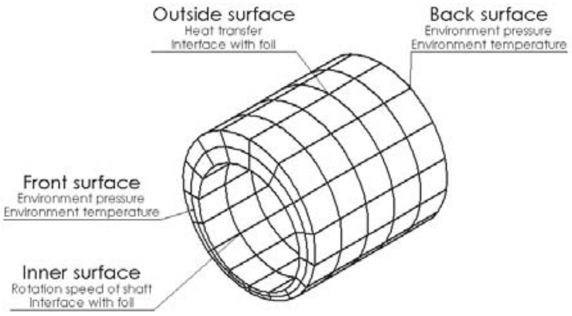

Fig. 3 Projective schematic of working fluid region in CFX module

C. Numerical Simulation Analysis Model of GFB in Foil Structure

After we build the fluid field analytical model of GFB by using the CFX module, the next step is to build a model to simulate the status of the characteristic of the foil structure and the shaft movement by using the transient structure module of Ansys. Similar to the method which we used to build the fluid field model, the foil structure and the shaft also take a hollow circle column 3D geometry model to simulate the shape for the foil structure and the shaft of GFB. From the point of view of the foil structure, due to directly considering the state of reality, the arrangement of top foil and bump foil is too complicated to mesh the structure. Hence, we will consider the homogeneous material structure which has the equivalent elastic characteristic to organize the analytical model of foil structure. That kind of setting is more practical not only for the simulation, but also for reducing the calculation time for analysis of the simulation process of the model. Therefore, the 3D geometry model of the foil structure combined by top foil and bump foil can be directly built by connecting two hollow circle column 3D geometry models and setting material properties for top foil and bump foil individually. On the other hand, the shaft will be supported by the extra pressure, which is produced from the fluid being dragged by the shaft surface. That effect will force the fluid to go through the compression and expansion process in the clearance between the top foil and shaft surface. However, the direction of the summation of support forces caused by that effect will not pass through the center of the shaft. As a result, the shaft will start a certain revolution motion centered somewhere in the bearing hole. That path of the shaft traveling in the bearing hole is a very critical factor of most applications of GFB. Because of that, the effect will directly decide whether the shaft will collide with the top foil or not. Taking one step further, due to the vibration feature of the foil structure, it will be directly caused by the motion of the shaft. It allowed designers to even estimate the service life of the bearing system for the simulation model. To achieve the goal of estimating the path of shaft revolution motion, we directly built a hollow circle column 3D geometry model and set material properties for the shaft. It was noteworthy that the value of inertial mass and gravitational field strength of the shaft should be set for a pair in coordination. Therefore, we could avoid incorrectly solving the motion of the shaft because of the wrong acceleration result, see Fig. 4 for details.

D. Fluid-Structure Interaction Numerical Simulation Model of GFB

After we built the fluid field analytical model and mechanical structure analytical model of GFB in Ansys, the multi-physics coupling simulation process during the data transmission of the different field interface calculation can be calculated. It can allow those two different models not only to achieve the result of transmission of analysis in each field but also the mesh displacement due to the finite element method process. Finally, this system coupling model could simulate the features of the whole bearing during operating, see Fig. 5 for details.

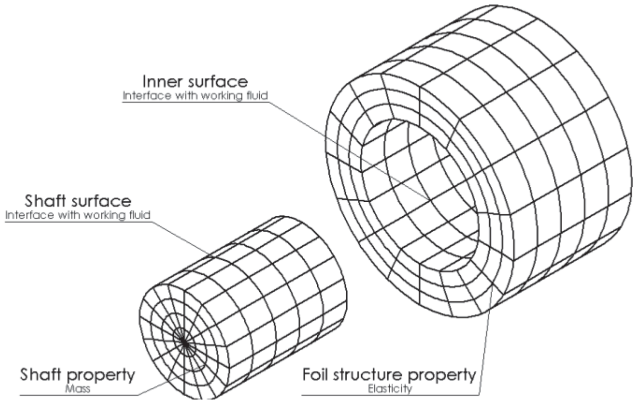

Fig. 4 Projective schematics of foil structure and shaft in Transient Structure module

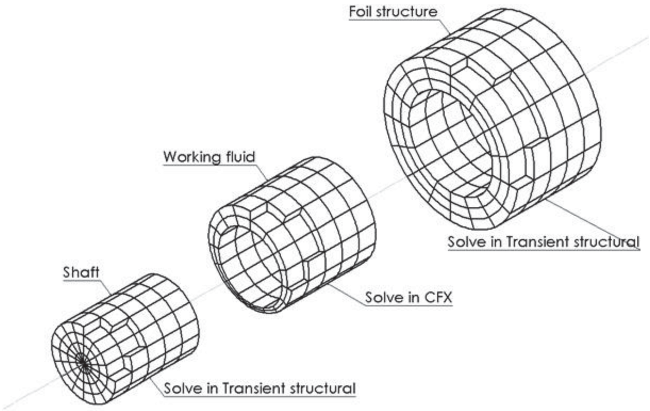

Fig. 5 Projective schematics including regions for of multi-domain coupling CAE simulations

III. RESULTS AND DISCUSSION

To simulate the operating situation of the GFB from start-up to stable working, we set the 3D geometry model of GFB in the initial state within eccentricity to be 0.8, which means to set a 1.5-inch (38.1 mm) diameter of shaft in 50 micrometer average clearance around the shaft. As a result, the minimum clearance setting in the bottom side of the shaft is 10 micrometer and the maximum clearance setting in the top side of the shaft is 90 micrometer, see Fig. 6 for details.

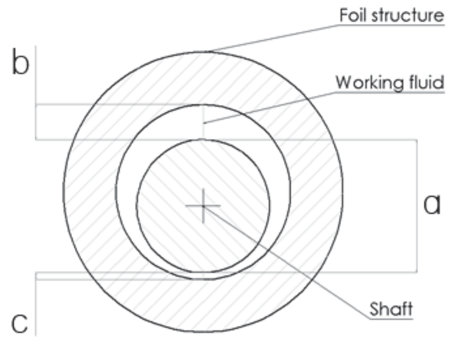

Fig. 6 Schematic to define the initial position of simulations model: a = 38.1 millimeter, b = 90 micrometer, c = 10 micrometer

While the simulation process gets started, the state of the working fluid of bearing which is in the clearance between the shaft and foil will be solved by the CFX module in Ansys. The process is based on the initial condition, which is set by the we, for example: the arrangement of pressure and temperature. After that, the result of the working fluid solved by the CFX model will be transferred to the model in the transient structural module as boundary and continue to do the analysis process. Therefore, the structural part in GFB will also be analyzed during a certain time interval which is set in the system coupling module of Ansys. Using the same method, after the process of analysis of transient structural module finishes, the result will be transferred back to the model in the CFX module as a boundary condition. The whole simulation will repeat this process again and again until the accumulated time step achieves a certain time, which is set in the program or the shaft collision to the top foil caused by shaft moving during the support force unbalanced in bearing. The initial condition is set in the CFX module and transient structural module, see Table I for details.

TABLE I
INITIAL CONDITION OF ANALYTICAL MODEL

Module	Factor	Value	Unit
CFX	Environment Pressure	1.0	Bar
CFX	Environment Temperature	303	K
CFX	Rotation Speed of shaft	6,000	rpm
CFX	Rotation Direction of shaft	Counterclockwise	NA
Transient Structural	Loading of shaft	1.0	N

After the simulation process of the multi-domain system coupling analysis procedure completes, we can confirm the pressure arrangement of working fluid, temperature arrangement of working fluid, revolution speed of the shaft, trajectory of the shaft center, displacement of foil structure or other factor relative to time scale in CFX module and transient structural user interface of Ansys. Observing those factors of bearing can allow to understand the situation of the bearing working, the property of bearing or even the method of adjusting the property of bearing for the next generation.

As a result, we could understand the working fluid property in each time interval while the GFB is operating by directly checking the result data in the post processing software interface.

TABLE II
MAXIMUM AND MINIMUM VALUES OF SIMULATED PRESSURE AND TEMPERATURE WHEN THE SHAFT IS AT VARIOUS POSITIONS

Position	Max. Pres. (bar)	Min. Press. (bar)	Max. Temp. (K)	Min. Temp. (K)
12	1.003	0.986	308.4	303.6
1.5	1.006	0.986	308.3	303.5
3	1.010	0.986	308.2	303.5
4.5	1.018	0.994	307.9	303.5
6	1.023	0.999	307.7	303.5
7.5	1.017	0.996	307.2	303.4
9	1.010	0.994	307.4	303.4
10.5	1.001	0.991	307.8	303.7

From Figs. 7-14, plots of contour maps indicating working fluid states expressed in pressure and temperature are illustrated when the rotating shaft is at various position as clock needle directions. And, the corresponding maximum and minimum pressure and temperature values are given in Table II to show the peak values of the states.

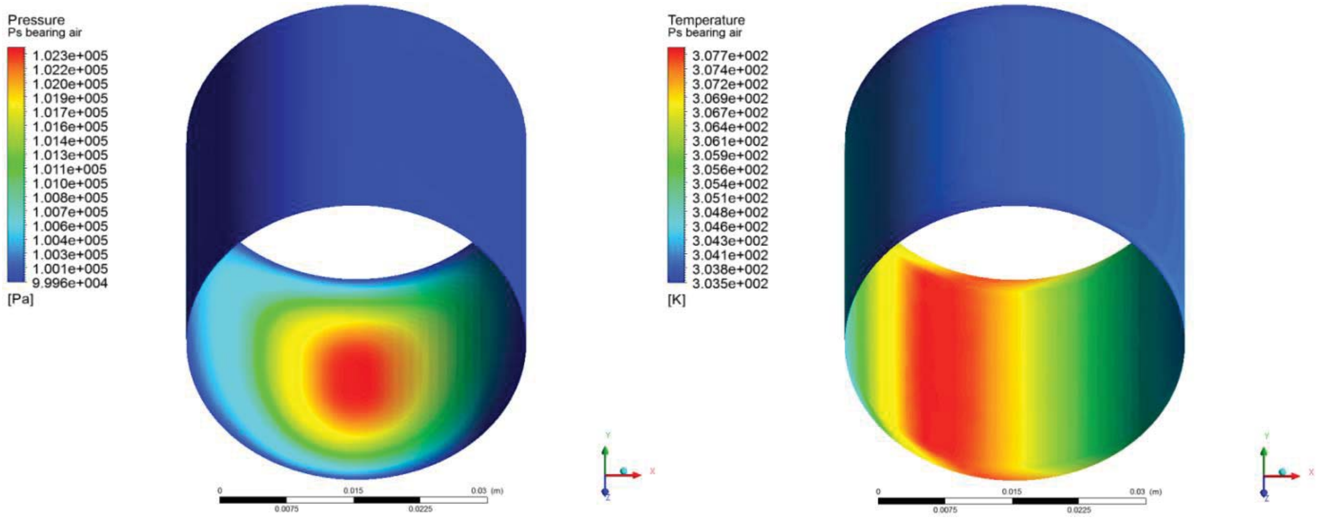

(a) pressure arrangement (b) temperature arrangement

Fig. 7 3D contour map of working fluid states when the shaft being at 6 o’clock position

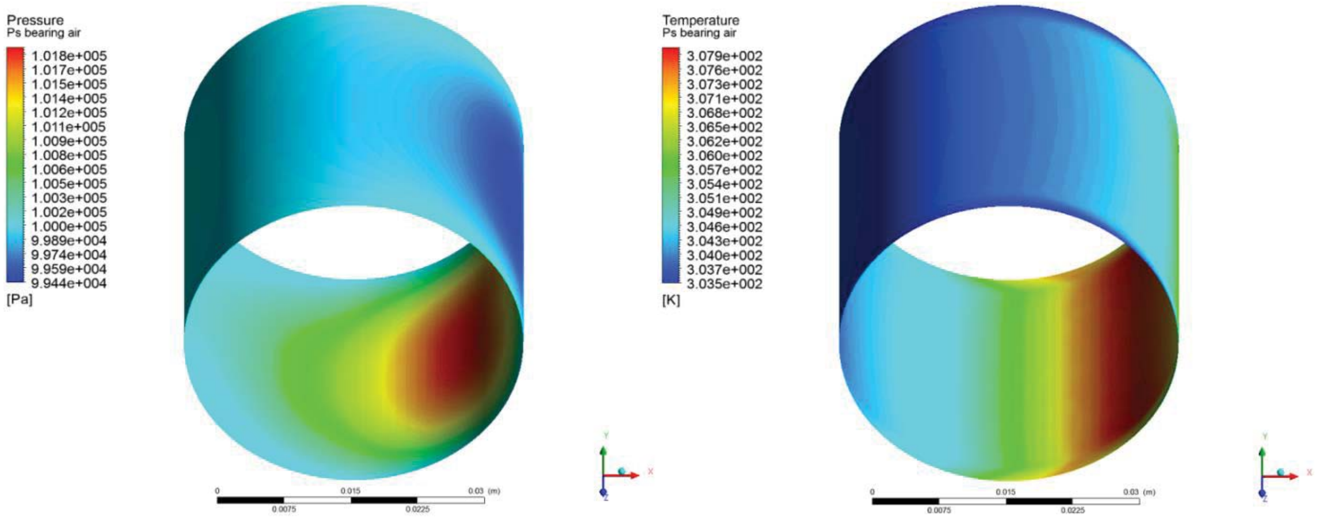

(a) pressure arrangement (b) temperature arrangement

Fig. 8 3D contour map of working fluid states when the shaft being at 4.5 o’clock position

In the simulations, the shaft starts at the initialized position with given rotational speed; then, the shaft reaches steady state after the pressure and temperature of the air film are established in convergent conditions. Hence, the shaft rotates smoothly under stable closed-loop motions with very small planetary oscillations. Fig. 15 shows the convergent shaft center trajectory starting initially at 6 o’clock position. It is noted that the shaft has reached stable rotational motions given the initial and boundary conditions of the CAE simulations. Therefore, the trajectory of the shaft center repeatedly traces same circular path in stable operation condition. After that, Fig. 16 shows the relationship between the speed of revolution of the shaft and time. By observing Fig. 16, we can understand that though the speed increased rapidly when the working of the shaft was just getting started, after it achieved the certain speed bearing became stable and achieved a certain working situation. After that, Fig. 17 shows the relationship between the displacement of top foil at the bottom of bearing and time. The observations of Fig. 17 can assist us to understand the period of the shaft revolution during working in the GFB of this simulation model.

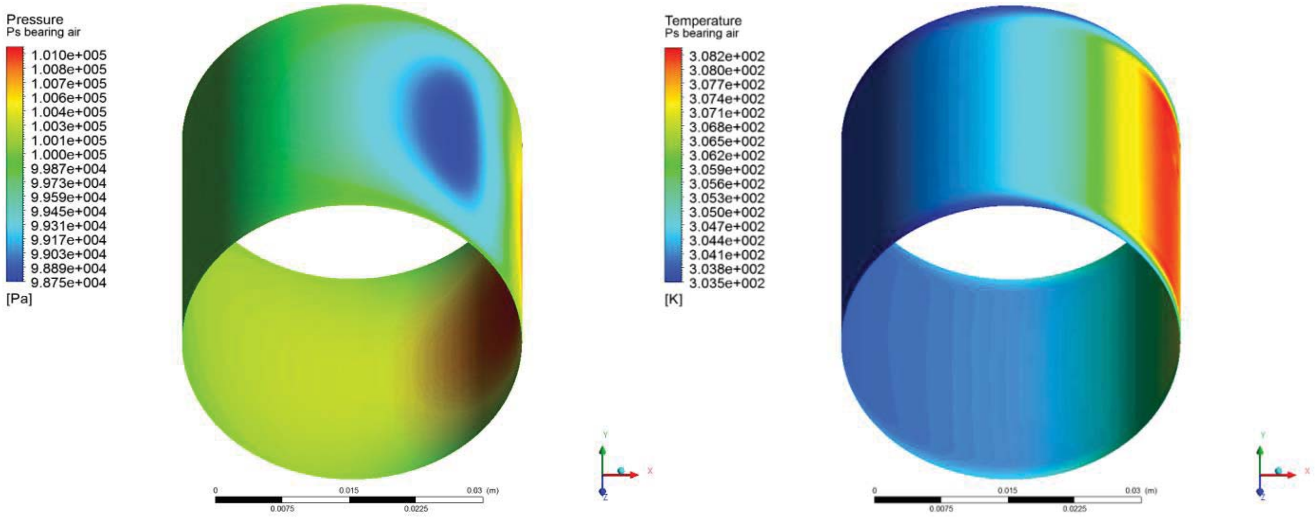

(a) pressure arrangement (b) temperature arrangement

Fig. 9 3D contour map of working fluid states when the shaft being at 3 o'clock position

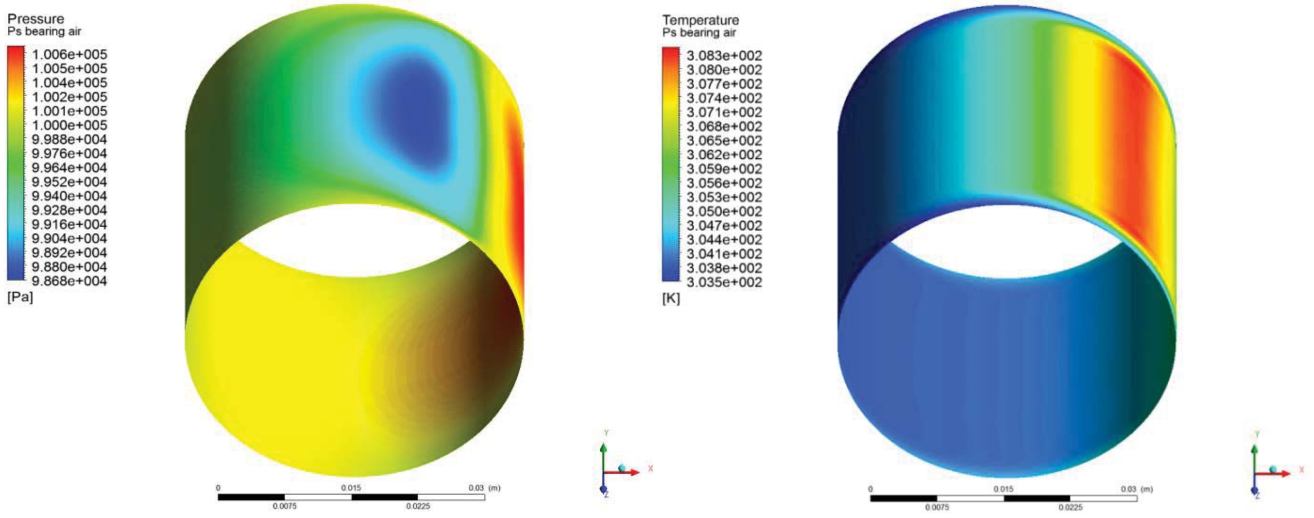

(a) pressure arrangement (b) temperature arrangement

Fig. 10 3D contour map of working fluid states when the shaft being at 1.5 o'clock position

Fig. 18 shows the relationship between the speed of top foil at the bottom of bearing and time. The observation of Fig. 18 can assist us to understand the pattern of the foil structure motion during working in the GFB of this simulation model. If we compare Fig. 18 with Fig. 17, it can be seen that every time the position of the shaft returns to the bottom of the bearing hole, the vibration speed of the bottom foil will suddenly change. Otherwise, the foil will just remain in slight vibration. This phenomenon is considered when the shaft moves close to a certain position of the foil causing it to be pulled close to the shaft resulting from the tension force in the foil structure, thus changing the shape of foil to carry the shaft. Every foil structure set around the inner side of the bearing will repeat this motion sequentially to let the GFB work smoothly, see Fig. 18 for details.

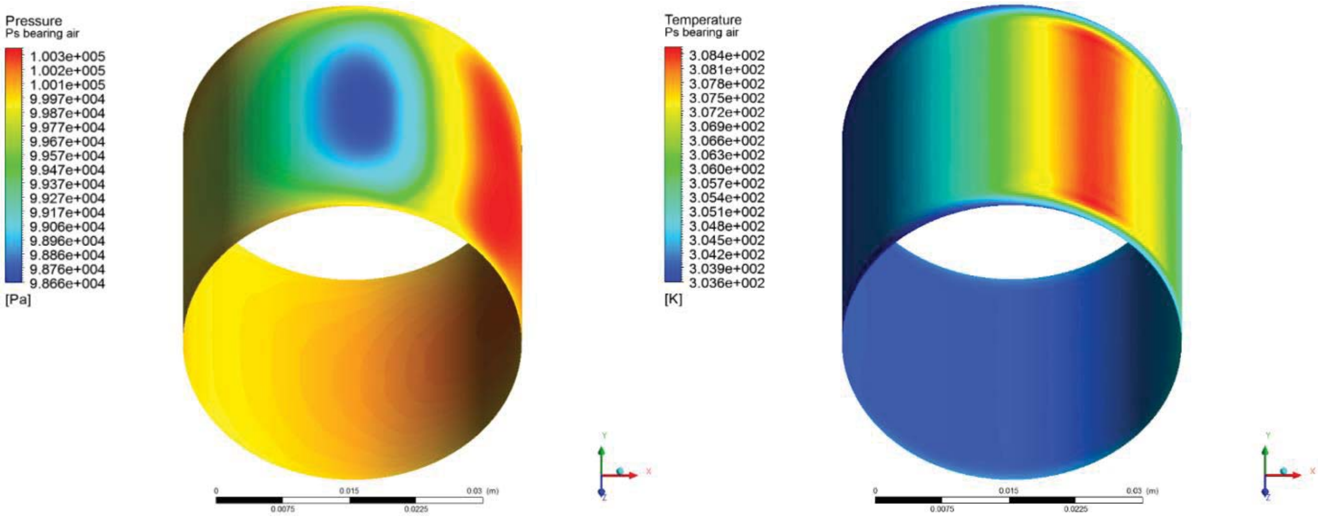

(a) pressure arrangement (b) temperature arrangement

Fig. 11 3D contour map of working fluid states when the shaft being at 12 o'clock position

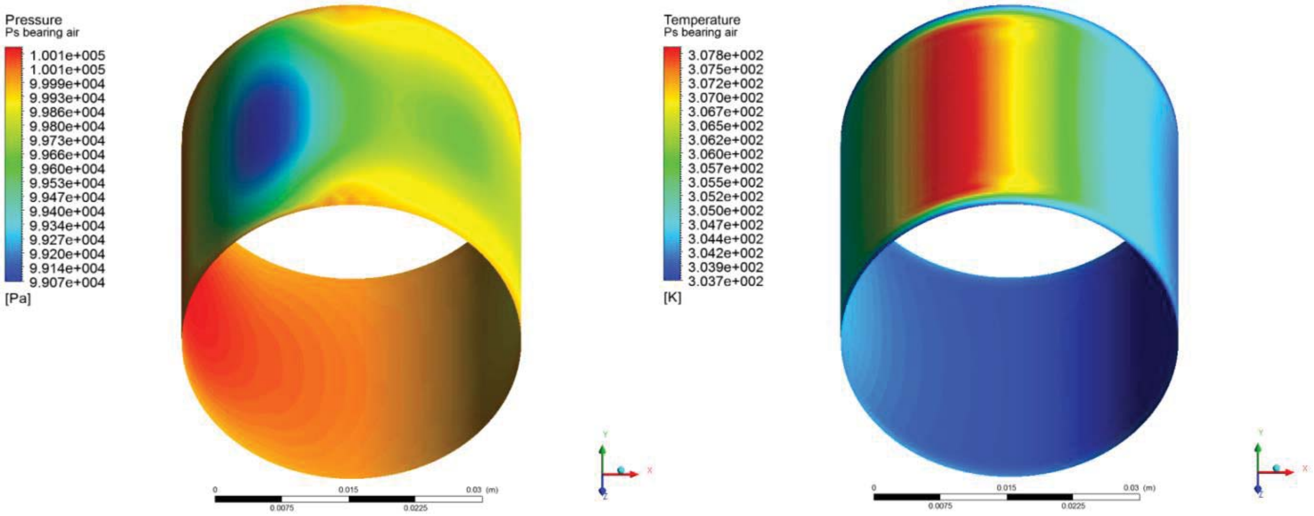

(a) pressure arrangement (b) temperature arrangement

Fig. 12 3D contour map of working fluid states when the shaft being at 10.5 o'clock position

IV. CONCLUSION

In this paper, a simulation scheme of rotational motions for predicting bump-type GFBs operating at steady-state is investigated. The scheme is based on commercial multi-physics coupling CAE programs, copyrighted by Ansys Inc., USA, modularized with computational fluid dynamics model and structure elasticity model to numerically co-simulate the dynamic equation of motions of a hydrodynamically loaded rotating shaft supported by bump foil structure.

In the simulations, stable planetary rotational motions of the loaded shaft are observed with output plots with pressure and temperature contour maps. The results indicate that successful simulation results can be obtained with the proposed scheme with the appropriate boundary and initial conditions on the shaft and foils. It is also noted that if load on the shaft exceeds the design limits, the shaft will contact the foil surface and simulation program will crash with error messages.

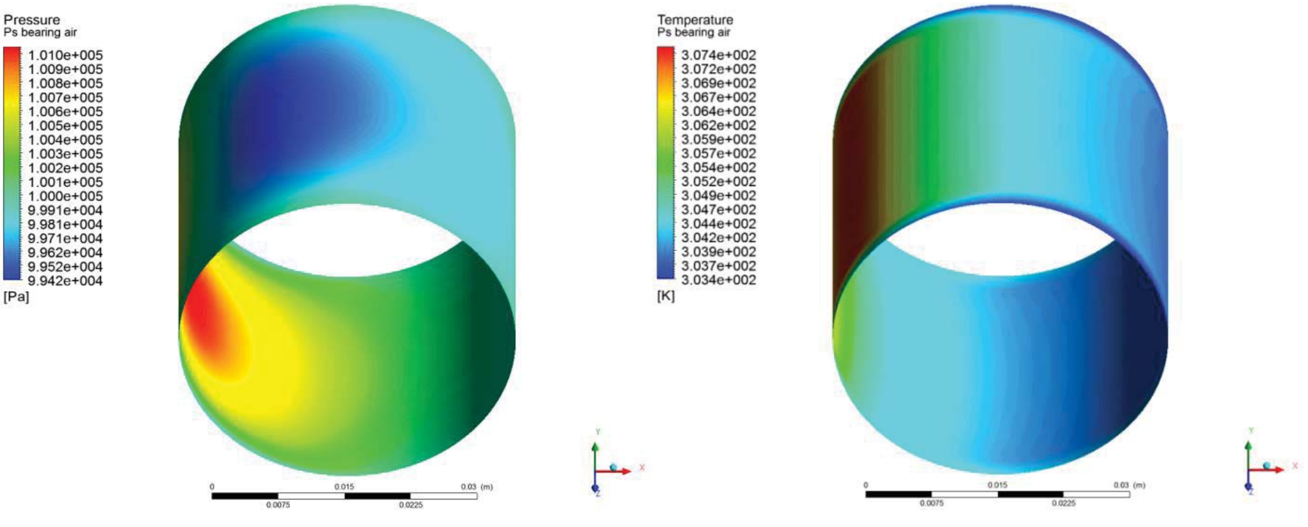

(a) pressure arrangement (b) temperature arrangement

Fig. 13 3D contour map of working fluid states when the shaft being at 9 o’clock position

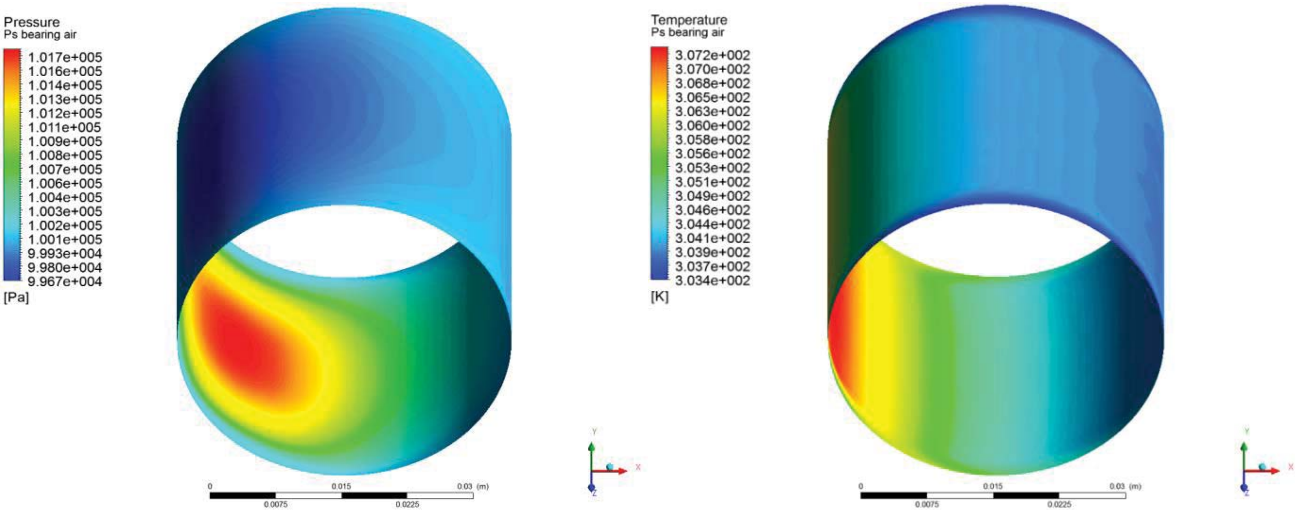

(a) pressure arrangement (b) temperature arrangement

Fig. 14 3D contour map of working fluid states when the shaft being at 7.5 o’clock position

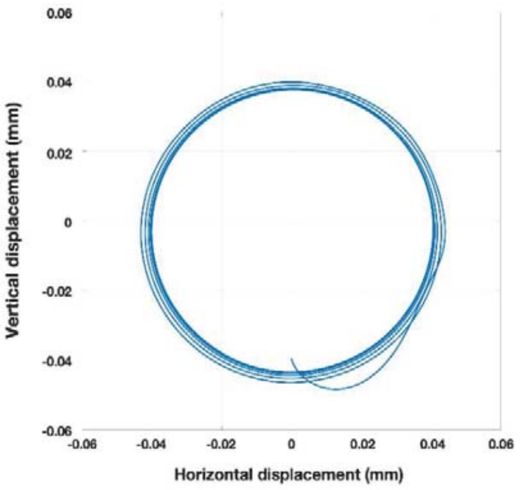

Fig. 15 Simulated shaft center motion of trajectories indicating the convergence of trajectory to a stable periodic loop

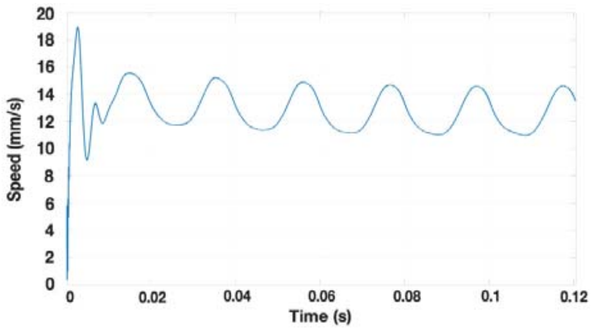

Fig. 16 Simulated shaft center revolution speed in planetary motion approaching stable periodic loop

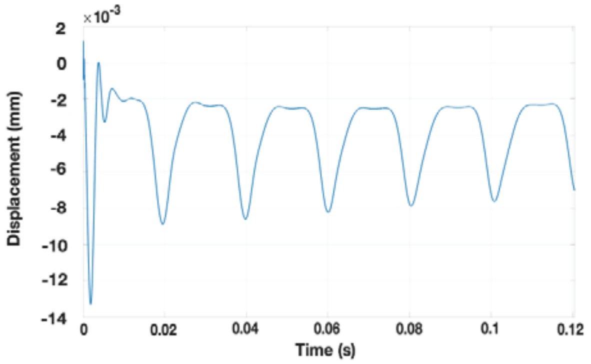

Fig. 17 Simulated top foil displacement at location defined in the 6 o'clock direction; periodic motion also being observed

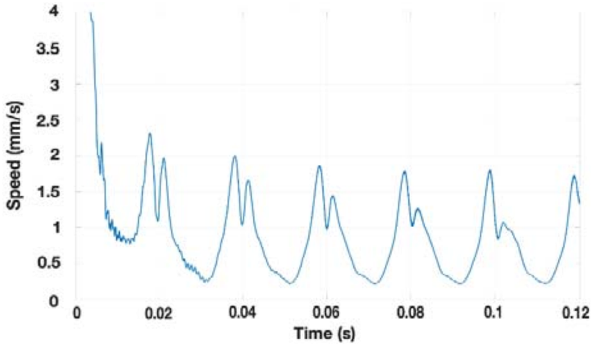

Fig. 18 Simulated top foil velocity at location defined in the 6 o'clock direction; periodic motion also being observed

Conclusively speaking, steady-state performance of GFBs can be simulated with the help of multi-physics coupling analysis commercial packages conducted on PC equipped with appropriate computation resources. The simulated results could be employed for experimental verifications published elsewhere with detailed information such as states of working fluid and stress and strain values in the foils. It would be interesting if further studies on the modeling of fiction forces and cross flow in gas film can be conducted in the future together with experimental verifications on the operating performances of GFBs.

REFERENCES

[1] Walowit, J. A., and Anno, J. N., "*Modern Developments in Lubrication Mechanics, Applied Science*", London, (1975), Chap. 7.
[2] Heshmat, H., Walowit, J. A., and Pinkus, O., "Analysis of Gas-Lubricated Foil Journal Bearings," *ASME J. Lubr. Technol.*, 105, (1983), pp. 647–655.
[3] Ku, C. P., and Heshmat, H., "Compliant Foil Bearing Structure Stiffness Analysis: Part I—Theoretical Model Including Strip and Variable Bump Foil Geometry," *ASME J. Tribol.*, 114, (1992), pp. 394–400.
[4] Agrawal, G. L., "Foil Air/Gas Bearing Technology—An Overview," *ASME Paper No. 97-GT-347*. (1997).
[5] Iordanoff, I., "Analysis of an Aerodynamic Compliant Foil Thrust Bearing: Method for a Rapid Design," *ASME J. Tribol.*, 121, (1999), pp. 816–822.
[6] DellaCorte, C., and Valco, M. J., "Load Capacity Estimation of Foil Air Journal Bearings for Oil-Free Turbomachinery Applications," *NASA/TM, Report No. 2000-209782.*, (2000).
[7] Carpino, M., and Talmage, G., "A Fully Coupled Finite Element Formulation for Elastically Supported Foil Journal Bearings," *Tribol. Trans., 46, (2003)*, pp. 560–565.
[8] Peng, Z.-C., and Khonsari, M. M., "Hydrodynamic Analysis of Compliant Foil Bearings with Compressible Air Flow," *ASME J. Tribol.*, 126, (2004), pp. 542–546.
[9] Peng, Z. C., and Khonsari, M. M., "A Thermohydrodynamic of Foil Journal Bearings," *ASME J. Tribol.*, 128, (2006), pp. 534–541.
[10] Swanson, E. E., "Bump Foil Damping Using a Simplified Model," *ASME J. Tribol.*, 128, (2006), pp. 542–550.
[11] San Andres, L., and Kim, T. H., "Improvements to The Analysis of Gas Foil Bearings: Integration of Top Foil 1D and 2D Structural Models," *ASME Paper No. GT 2007-27249*. (2007).
[12] Le Lez, S., Arghir, M., and Frene, J., "A New Bump-Type Foil Bearing Structure Analytical Model," *ASME J. Eng. Gas Turbines Power*, 129_4_, (2007), pp. 1047–1057.
[13] Le Lez, S., Arghir, M., and Frene, J., "Static and Dynamic Characterization of a Bump-Type Foil Bearing Structure," *ASME J. Tribol.*, 129, (2007), pp. 75–83.
[14] Feng, K., and Kaneko, S., "A Numerical Calculation Model of Multi Wound Foil Bearing with the Effect of Foil Local Deformation," *Journal of System Design and Dynamics*, JSME, 1, (2007), pp. 648–659.
[15] Lee, Y., Park, D., Kim, C. H., and Kim, S. J., "Operating Characteristics of the Bump Foil Journal Bearings with Top Foil Bending Phenomenon and Correlation Among Bump Foils," *Tribol. Int.*, 41, (2008), pp. 221–233.